

EFFECT OF CLUSTERING UPON A 500-MB. HORIZONTAL SOUNDING SYSTEM¹

J. K. ANGELL AND W. A. HASS

Environmental Science Services Administration, Washington, D.C.

ABSTRACT

Stream functions and velocity potentials derived from historical tapes of the National Meteorological Center are utilized to provide an estimate of the degree of clustering to be expected from a 500-mb. horizontal-sounding system. From a basically symmetric distribution of particles (balloons) over the Northern Hemisphere north of 15° N., it is found that the clustering tendency increases for 25 days after trajectory initiation and then remains essentially invariant. Under the latter condition the particle density is twice the initial density over 5 percent of the Northern Hemisphere, and is less than one-quarter the initial density over a similar area. Comparison with synoptic maps shows that clustering tends to be associated with ridges in the 500-mb. flow pattern and as a result, in the mean, clustering is most pronounced over western North America and western Europe. Clustering also tends to occur in areas of weak pressure gradient. Dispersion statistics derived from the particle trajectories imply a lateral standard deviation proportional to approximately the 0.5 power of the downwind distance and a value of about 2×10^{10} cm.² sec.⁻¹ for the (lateral) eddy diffusivity. The data coverage to be anticipated from constant volume balloon launch sites in Japan is discussed briefly.

1. INTRODUCTION

The problem of obtaining meteorological information in the free atmosphere at intervals of a few hundred kilometers on a global basis has recently become important because of the capability of electronic computers to utilize such information in a meaningful fashion. One of the methods of obtaining such information involves the use of satellites to position constant volume balloons, and to store the data obtained therefrom (Lally [1]). Of basic importance to this concept is the degree to which the free-floating balloons would cluster in certain areas, leaving other areas devoid of balloons and hence of meteorological information. If the clustering is very pronounced, the cost and logistics of releasing additional balloons to fill the data gaps might make the concept unfeasible. The primary purpose of this paper is to estimate the degree of clustering which might be expected at 500 mb. and to determine those areas where, on the average, additional constant volume balloons might have to be released in order to maintain the desired data density. In addition, certain dispersion statistics of meteorological interest are presented.

2. PROCEDURES

The historical data tapes stored at the National Meteorological Center (NMC) of the U.S. Weather Bureau contain, among other parameters, stream functions and velocity potentials at grid intervals of about 350 km., where the non-divergent component of the wind has been derived from the balance equation and a Poisson equation has been solved for the irrotational component.

Addition of these non-divergent and irrotational fields is assumed to yield the (divergent) wind field. Since the above data were not in chronological order (each tape contained data for one week at either 0000 or 1200 GMT), for purposes of a trajectory program it was necessary to sort and merge the data. This was accomplished with some difficulty because of a change in the method of storing the data during the period of study extending from June 1962 through February 1964.

The first attempt at a 500-mb. trajectory program was Lagrangian in the sense that it involved the use of a simple advective equation to deform the initial checkerboard grid by means of the winds at the grid points. This method worked well for about three days but thereafter the grid became so distorted that it proved impossible to identify specific grid intersections. Furthermore, it became apparent that truncation effects were producing instabilities in the computation procedure. It was therefore necessary to use an essentially Eulerian method which involved the displacement of particles initially at grid intersections by means of winds linearly interpolated to the subsequent positions of the particles. Since the particles were displaced in 1-hr. time steps, a linear interpolation in time was also required. This procedure was satisfactory in that stability was achieved for the desired time period, and furthermore, basic agreement was obtained with trajectories determined manually by means of the central tendency method. Nevertheless, it is unfortunate that constant volume balloons were not flown at the 500-mb. surface during this period, since comparison with real trajectory data would represent the definitive test.

There were three drawbacks to the above procedure and

¹This work was supported in large part by the National Environmental Satellite Center.

the method of utilization. First, trajectory interpolation proved not to be feasible and hence if either the stream function field or the velocity potential field was missing for one 12-hr. period, the trajectory computation had to be terminated. Inasmuch as it was desired to run the trajectories for 60 days (an estimate, perhaps an underestimate, of the lifetime of present-day constant volume balloons), the choice of starting dates was severely limited. However, it was possible to find periods during the winter of 1962-63 and during the summer and fall of 1963 when 60-day trajectories could be determined for 8 different starting times spaced 5 days apart. Unfortunately, no such period could be found during the spring of 1963. A second, and more serious, drawback involved the fact that no provision was made to replenish the particles which passed equatorward of the southern boundary of the NMC grid, as has been done, for example, by Mesinger [2]. The necessity of dealing with a variable number of particles has introduced severe problems into many aspects of the analysis. The third factor (related to the second) involves the fact that the rectangular NMC grid, when overlaid on a polar stereographic map projection, results in a greater density of grid intersections (particles) in tropical regions than in polar regions. Thus, initially, the particle density slowly increased with decrease in latitude as far as latitude 15° N., and then became zero.

In order to facilitate the necessary manual computations, we have not utilized every NMC grid intersection in the following analysis, but rather have concentrated upon the subsequent distribution of 200 particles initially located at grid intersections approximately 1,000 km. apart (fig. 1). Moreover, since visual inspection of the subsequent particle distribution showed that clustering tended to take place on the scale of the long waves in the westerlies, in order to obtain a more representative clustering statistic, a count has been made of the number of particles within squares approximately 2,000 km. on a side (170 overlapped squares available). The results presented herein are based upon such a count for time periods up to 60 days after trajectory initiation.

Originally it was planned to carry out a clustering study at 200 mb. as well as at 500 mb. This has not been accomplished because of a scaling difficulty at the 200-mb. surface. Mesinger [2] has found evidence that the clustering tendency decreases with increase in height, presumably because of the pronounced deformation fields associated with the stronger winds at the upper levels. It is likely, therefore, that the 500-mb. statistics presented herein are intermediate to the statistics which would be obtained at 850 and 200 mb.

3. CLUSTERING STATISTICS

As discussed in the preceding section, in order to estimate the degree of clustering, we have chosen to start with a basically symmetric distribution of particles

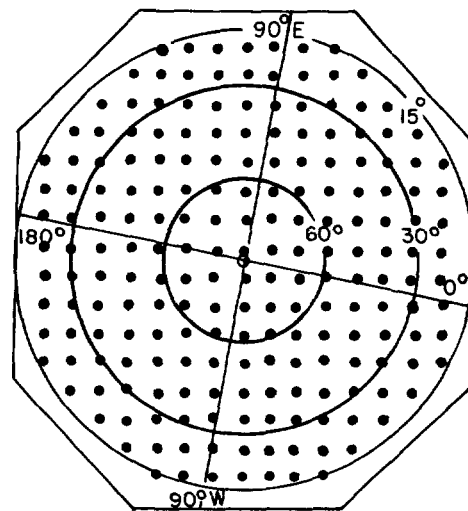
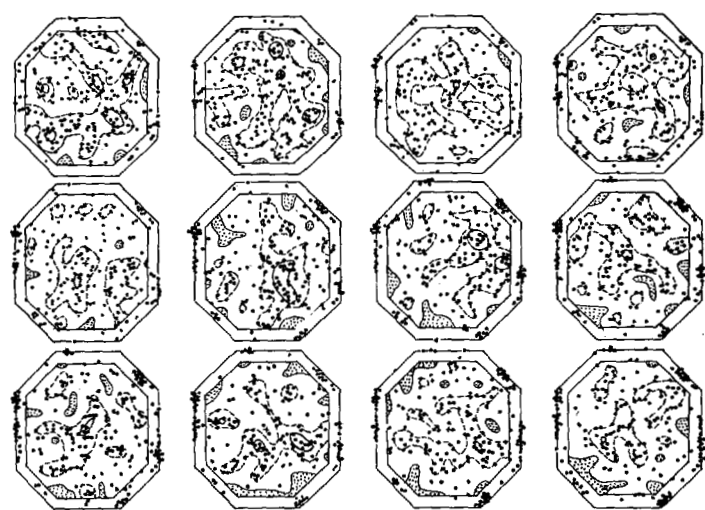


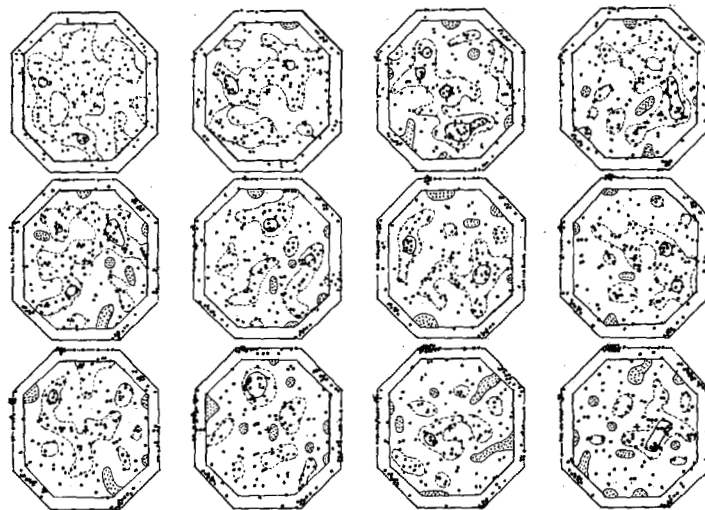
FIGURE 1.—Initial distribution of the 200 particles, based upon NMC grid intersections superimposed on a polar stereographic map projection.

(fig. 1) and to note how this distribution changed with time. Figures 2-25 show the distribution of particles 5-60 days after trajectory initiation for the 24 different starting dates during the three seasons. The dashed and solid isopleths show, respectively, where the particle density exceeds four and eight particles per 2,000-km. square; the stippling, the areas where no particles are to be found within a 2,000-km. square. The latter areas are mostly located near the equatorward limit of the NMC grid because of the particle loss to the Tropics. The top diagram of figure 26 shows the percentage of particles which passed equatorward of the NMC grid as a function of longitude. The percentage is at a maximum just to the east of the Greenwich Meridian (hence over North Africa), with a secondary maximum in the eastern North Pacific. It was in the latter area that transosondes, released from Japan for flight at 300 and 250 m.b. in winter, occasionally moved across the equator into the Southern Hemisphere (Angell [3]). The bottom diagram of figure 26 shows the difference in the above percentages between winter and summer. At all longitudes more particles pass equatorward of the NMC grid in winter than in summer, with the difference being greatest near 90° E. Presumably, this is a reflection of the strong monsoonal character of the flow in this region, and, in particular, of the movement of the jet stream south of the Himalaya Mountains in winter.

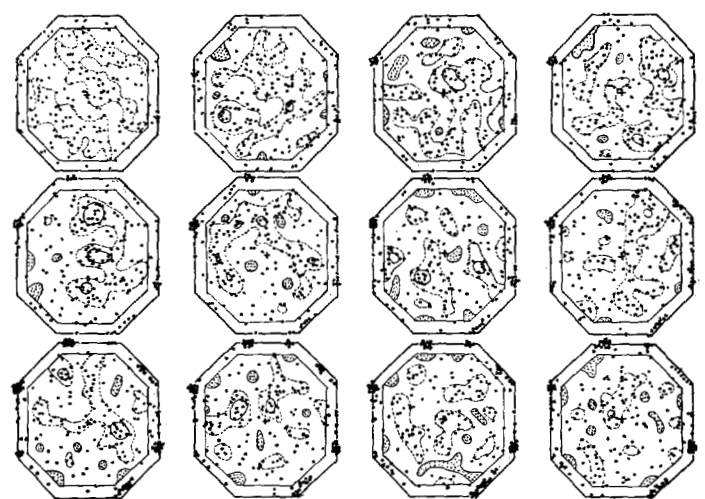
FIGURES 2-25.—For trajectory initiations on the given dates, the subsequent positions of the 200 particles at 5-day intervals from 5 to 60 days (reading from left to right and then down in each figure). The dashed and solid isopleths delineate, respectively, the areas where the particle density equals, and exceeds, a factor of two times the initial density; the stippling, the areas where no particles are to be found within a 2,000-km. square. Particles on the boundary are plotted where they passed equatorward of the NMC grid.



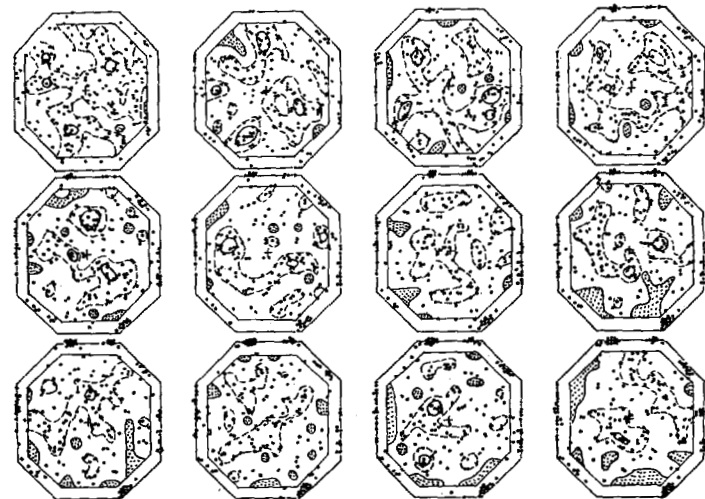
NOV. 4, 1962



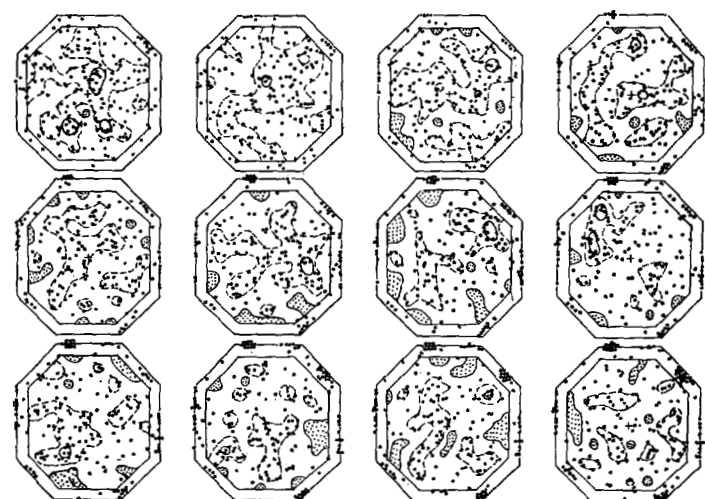
NOV. 19, 1962



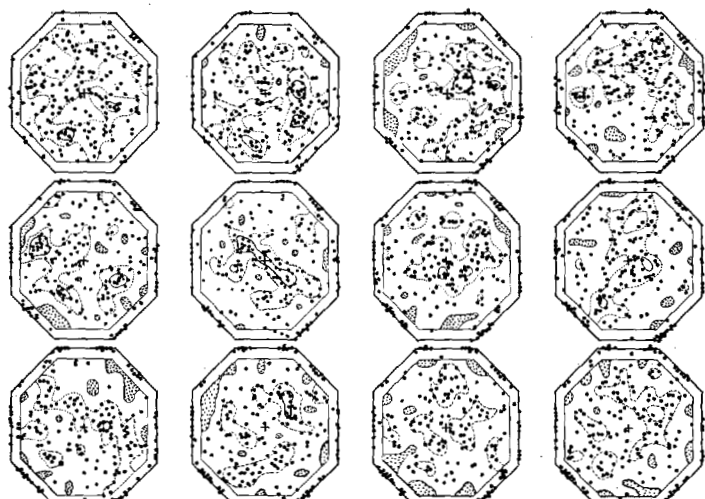
NOV. 9, 1962



NOV. 24, 1962



NOV. 14, 1962



NOV. 29, 1962

Figure 2.—November 4, 1962.
Figure 3.—November 9, 1962.
Figure 4.—November 14, 1962.

Figure 5.—November 19, 1962.
Figure 6.—November 24, 1962.
Figure 7.—November 29, 1962.

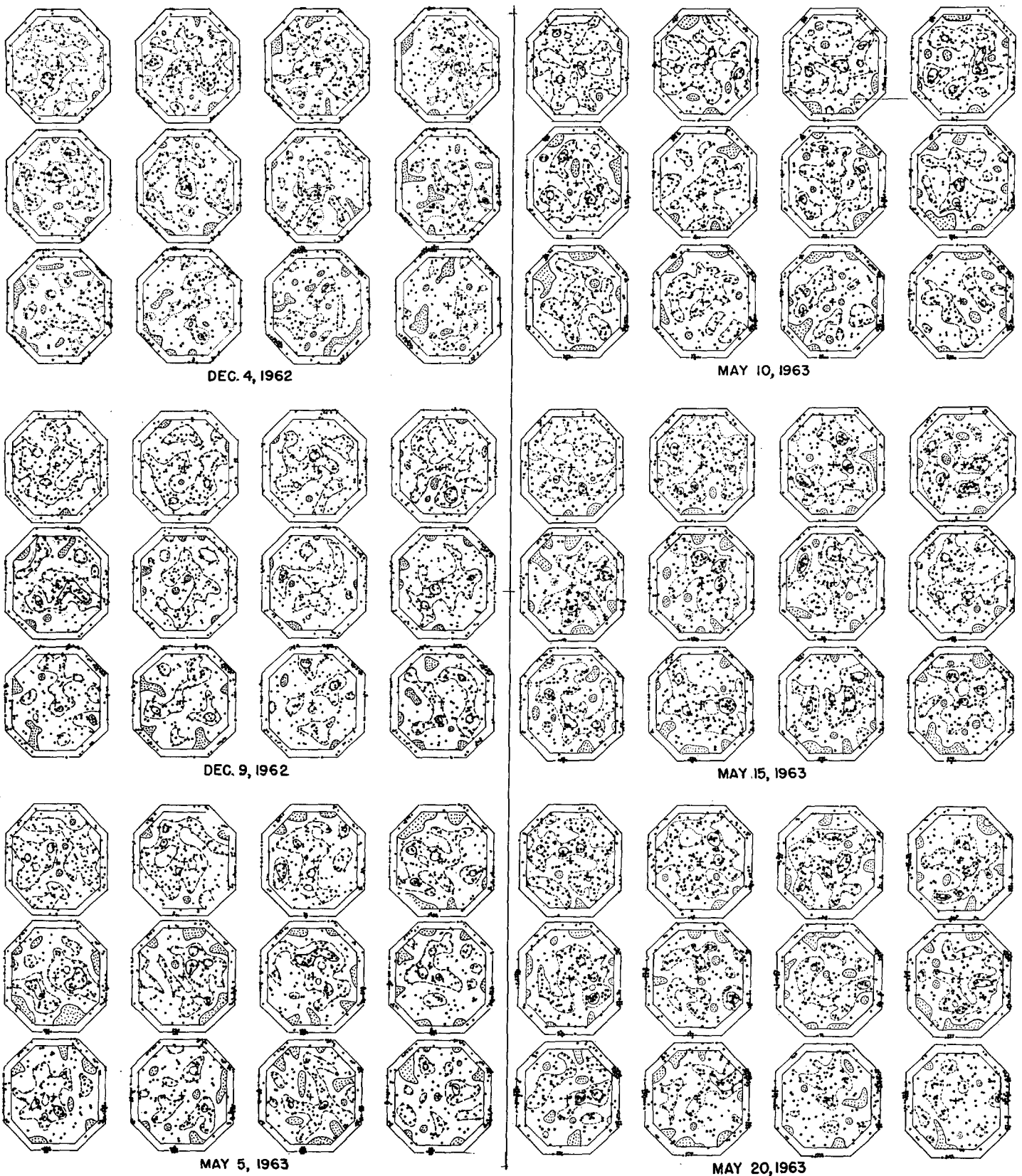
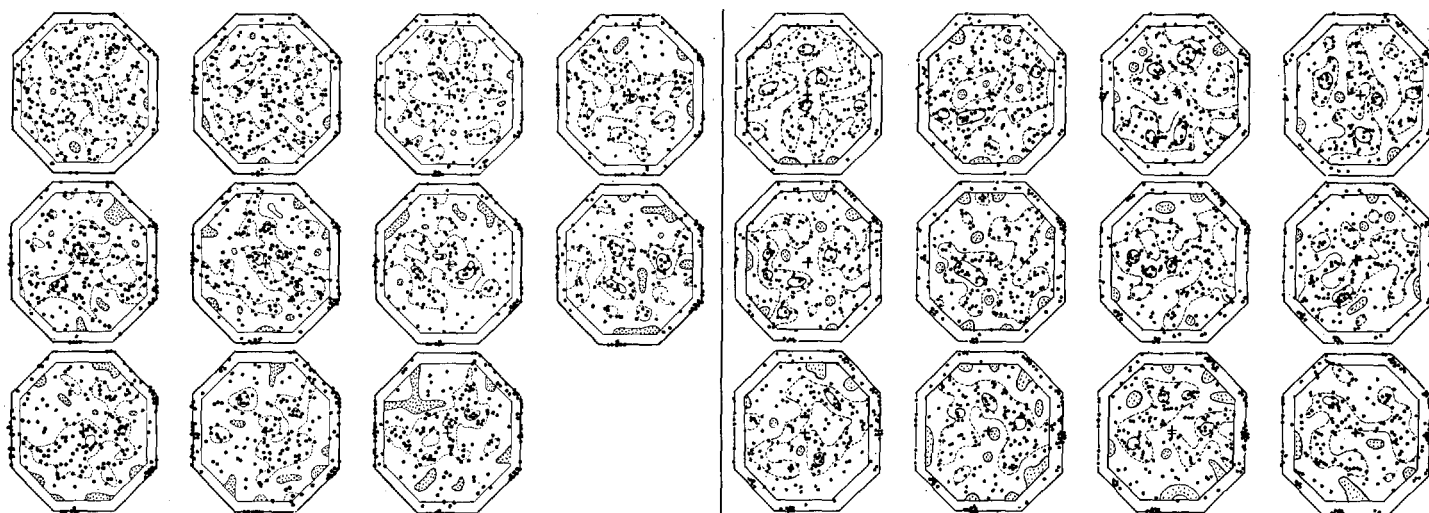


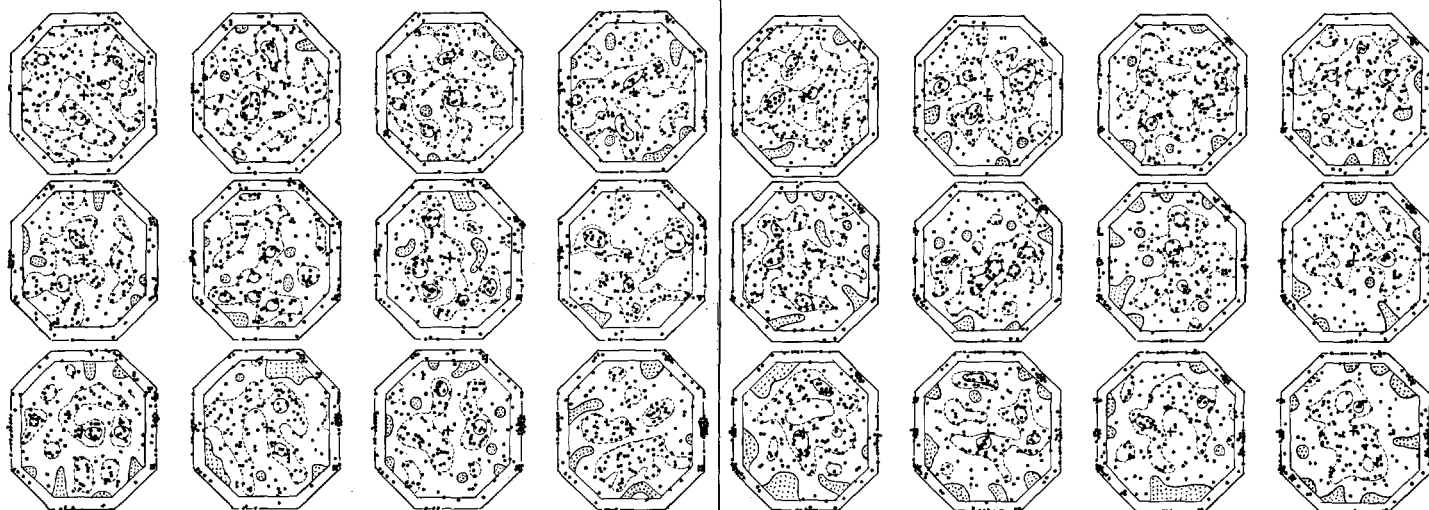
Figure 8.—December 4, 1962.
Figure 9.—December 9, 1962.
Figure 10.—May 5, 1963.

Figure 11.—May 10, 1963.
Figure 12.—May 15, 1963.
Figure 13.—May 20, 1963.



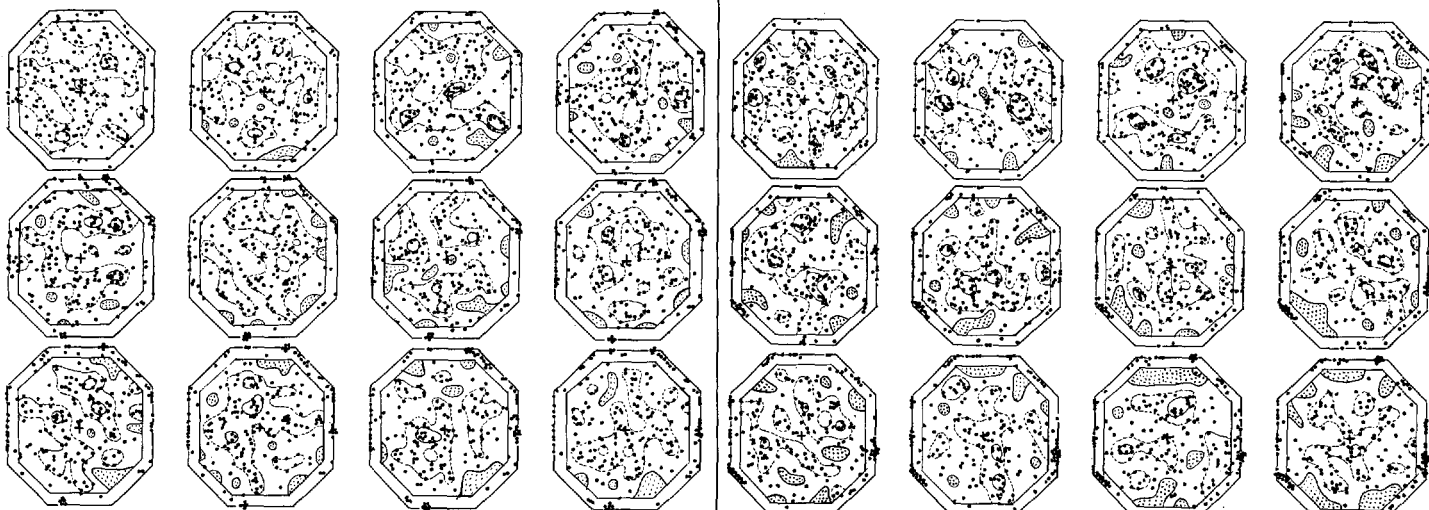
MAY 25, 1963

JUN. 9, 1963



MAY 30, 1963

SEPT. 7, 1963



JUN. 4, 1963

SEPT. 12, 1963

Figure 14.—May 25, 1963.

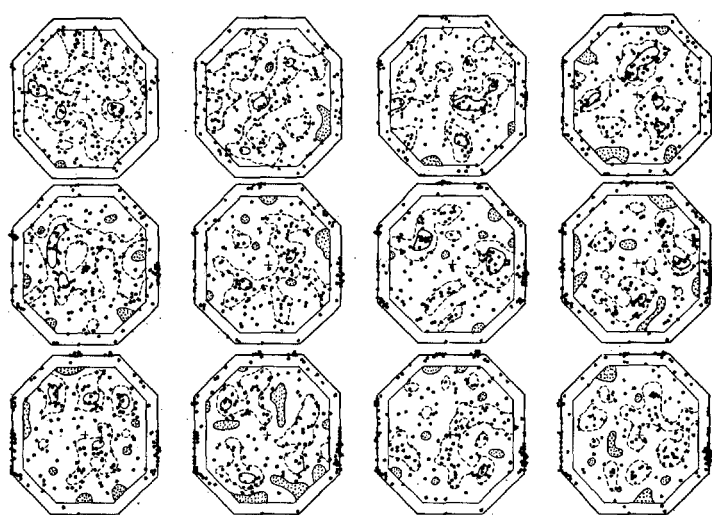
Figure 15.—May 30, 1963.

Figure 16.—June 4, 1963.

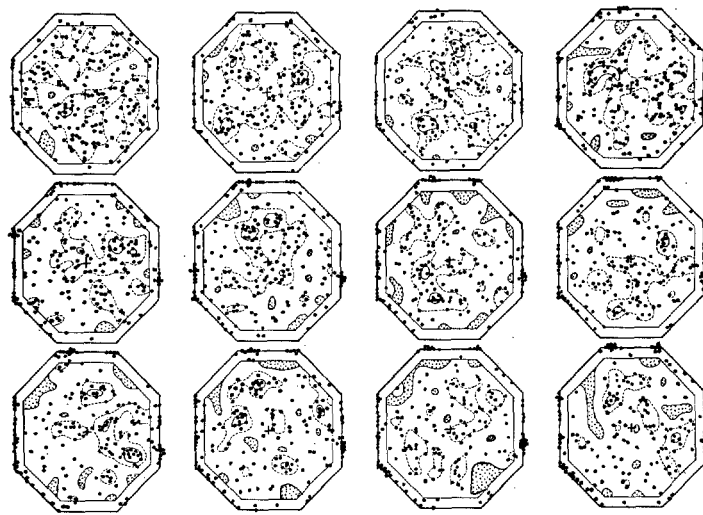
Figure 17.—June 9, 1963.

Figure 18.—September 7, 1963.

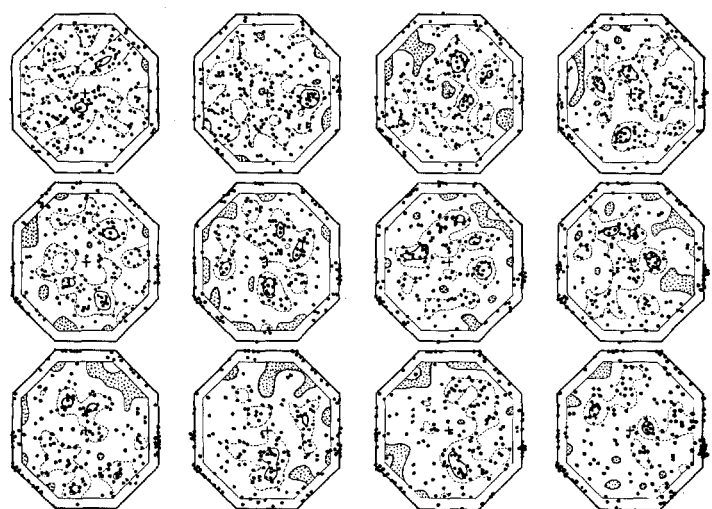
Figure 19.—September 12, 1963.



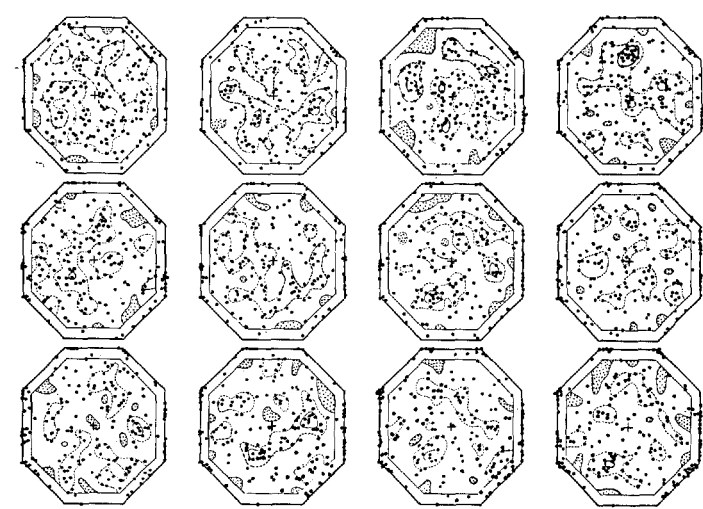
SEPT. 17, 1963



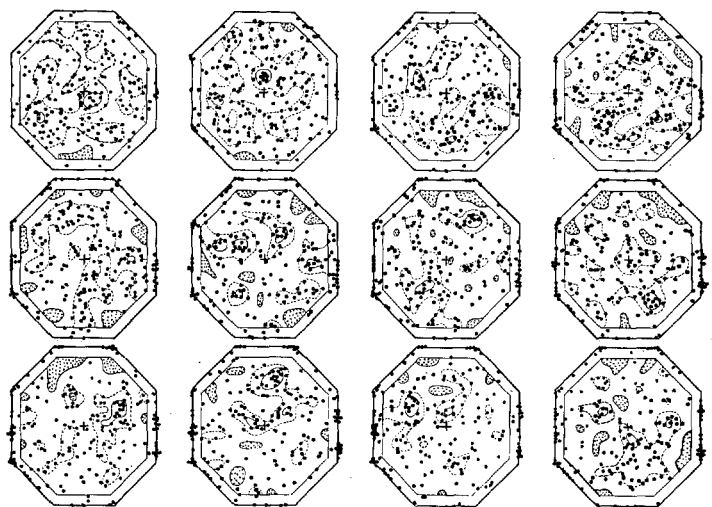
OCT. 2, 1963



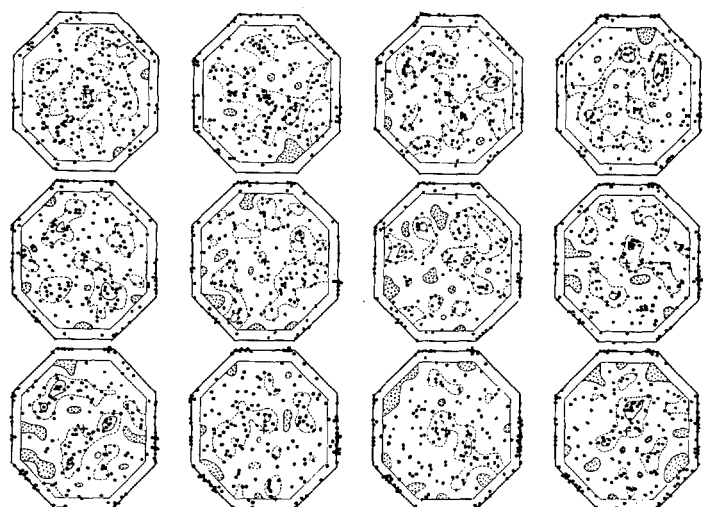
SEPT. 22, 1963



OCT. 7, 1963



SEPT. 27, 1963



OCT. 12, 1963

Figure 20.—September 17, 1963.
Figure 21.—September 22, 1963.
Figure 22.—September 27, 1963.

Figure 23.—October 2, 1963.
Figure 24.—October 7, 1963.
Figure 25.—October 12, 1963.

While in many ways figures 2-25 provide a better estimate of the degree of clustering than any statistic, a numerical measure of the extent of clustering is useful. Unfortunately, the continuous loss of particles to the Tropics (table 1) introduces complications into the statistical procedures. In order to correct for the decrease in the number of particles with time we have made the assumption that the "lost" particles, if they were still within the grid, would be distributed in proportion to the number of squares possessing a given number of particles. For example, if 60 squares had 3 particles each, 70 squares had 4 particles each, and 40 squares had 5 particles each (recall that, because of the overlapping squares, each particle is counted four times), then of the 20 lost particles (5 lost particles counted 4 times each), 60/170 or 35 percent would be placed in the squares possessing 3 particles, 70/170 or 41 percent in the squares possessing 4 particles, and 40/170 or 24 percent in the squares possessing 5 particles. Thus, with the assumption that only 1 "lost" particle would enter into any particular square, we would end up with 53 squares having 3 particles, 69 squares having 4 particles (gains 7 squares but loses 8 squares), 43 squares having 5 particles (gains 8 squares, loses 5 squares), and 5 squares having 6 particles. This procedure is probably satisfactory when only a few particles have been lost to the Tropics but it becomes more dubious when large numbers of particles have been lost, if only because of the assumption that no more than one lost particle enters into any particular square.

The (adjusted) number of squares possessing a certain particle count indicates directly the percentage area of the hemisphere over which a certain particle density might be expected. However, for a study of the variation in clustering as a function of time since trajectory initiation, it is desirable to have a single number represent the degree of clustering. The standard deviation of the number of squares possessing a given particle density is adequate for this purpose, since it is obvious that a large standard deviation would result from the combination of many squares with high and low particle density. It should be noted, however, that the standard deviation does have a theoretical drawback in that the above distribution is not truly Gaussian. The top diagram of figure 27 shows the average value of this standard deviation (hereafter denoted as

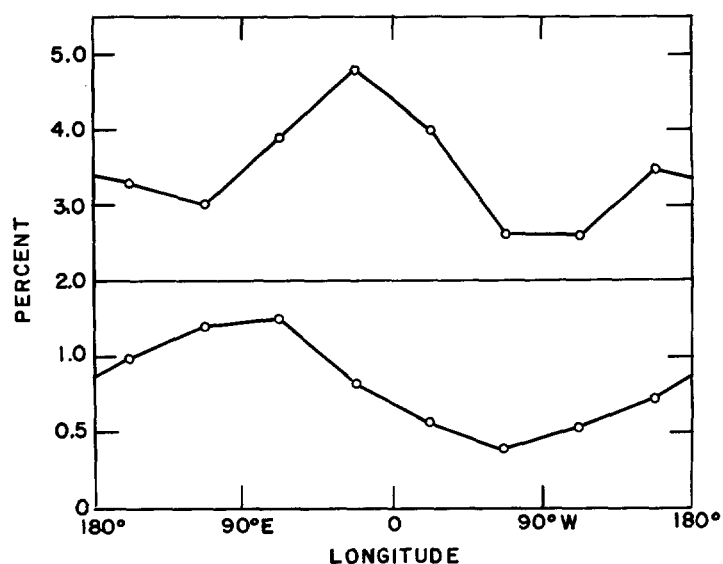


FIGURE 26.—Variation with longitude of the percentage of particles passing equatorward of the NMC grid within 60 days after trajectory initiation (top), and the difference, winter minus summer (bottom).

clustering index) as a function of time after trajectory initiation, based on all 24 starting dates. The clustering index increases for the first 25 days but thereafter remains practically constant. The slight decrease in the index after 50 days is probably not real but rather reflects a bias introduced into the statistics by the method of correction for particles lost to the Tropics. Thus, these data suggest that the divergences associated with synoptic-scale disturbances can produce only so much clustering (perhaps because of the declustering tendency induced by the field of deformation and by turbulence phenomena on all scales), and that, from a basically symmetric distribution of particles, the full extent of clustering is realized in about one month.

The bottom diagram of figure 27 shows the difference in clustering between summer and winter. For the first 15 days after trajectory initiation the clustering is slightly more pronounced in winter than in summer, presumably because of the larger divergences and convergences associated with the strong wintertime circulation. After 20 days, however, the clustering becomes somewhat more pronounced in summer than winter, chiefly because in

TABLE 1.—Percentage of the 200 particles which have moved equatorward of the NMC grid a given number of days after trajectory initiation

	Days											
	5	10	15	20	25	30	35	40	45	50	55	60
Winter.....	4.0	7.0	11.5	15.5	15.5	18.0	21.0	23.5	25.0	26.5	28.5	30.0
Summer.....	3.0	6.5	9.5	10.5	14.5	16.5	16.5	18.0	19.0	20.5	22.5	23.5
Fall.....	3.5	7.0	10.0	12.5	15.0	17.5	19.5	22.0	24.0	25.0	27.5	28.5

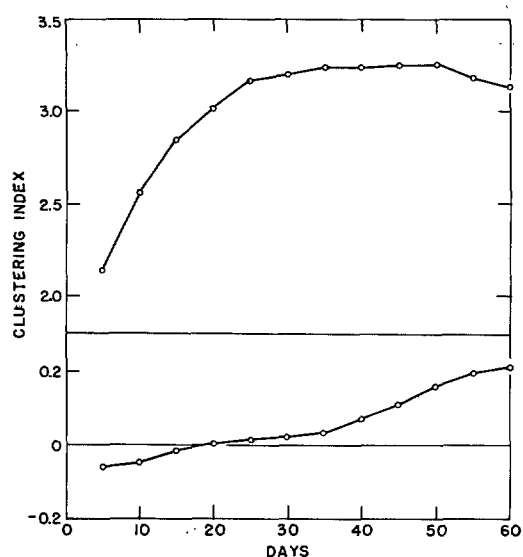


FIGURE 27.—Clustering index (standard deviation of the number of grid squares possessing a certain particle count) as a function of number of days after trajectory initiation (top), and the difference, summer minus winter (bottom).

summer the mean clustering index continues slowly to increase for 55 days after trajectory initiation.

Of greatest interest from the practical point of view of data coverage is the percentage area of the Northern Hemisphere (north of 20° N. in this case) over which, at any arbitrary time, one could expect the particle density to be less than or greater than the initial density. We believe the best estimate of this percentage area is obtained by averaging the results on particle density obtained 25, 30, and 35 days after trajectory initiation, since it has been shown that the clustering index varies little after 25 days, and yet prior to 35 days any bias introduced by our correction for the loss of particles to the Tropics should not be too serious (table 1). With this assumption, table 2 shows the percentage area of the Northern Hemisphere where, at any arbitrary time, the particle (constant volume balloon) density might be expected to exceed the initial density. The difference in seasons is not great, although, as mentioned in connection with figure 27, the clustering tendency is slightly more pronounced in summer than in winter. On the basis of table 2 one would estimate that over about 5 percent of the Northern Hemisphere the particle density might be expected to exceed twice the initial density and that over another 5 percent of the Hemisphere the particle density might be expected to be less than one-quarter the initial density. Furthermore, over 17–18 percent of the Hemisphere the particle density could be expected to be less than one-half of the initial density.

The percentages in table 2 are important in providing some idea of the average extent of the area over which, at any given time, the density of constant volume balloons might be expected to be deficient. As a corollary, they

TABLE 2.—Percentage area of the Northern Hemisphere (north of 20° N.) over which, at any arbitrary time, the particle (constant volume balloon) density might be expected to exceed the given factor of the initial density

Factor	Winter	Summer	Fall
0.25	95.1	93.7	94.8
0.50	82.9	81.3	82.7
1.00	45.2	46.4	45.9
1.50	16.0	18.1	17.0
2.00	4.2	4.5	5.0

yield an estimate of the balloon replacement rate needed to fill the data gaps. For example, if a balloon density of less than one-half the initial density was assumed to yield an area of serious data deficiency, then, with the given conditions, during the period of one month one would have to release approximately 36 (200×0.18) balloons to fill the data gaps. During the next month, to a first approximation, the procedure would have to be repeated, so that on the average over this 60-day period approximately one balloon would have to be released each day. Accordingly, for the assumed lifetime of the balloons (60 days), the initial number of balloons would have to be augmented by about one-third in order to maintain the requisite data density, neglecting, of course, the balloon attrition due to other causes. With some rather dubious assumptions, this factor of 30 percent might also be considered the percentage of additional balloons one should release initially in order to insure that data gaps did not develop for the lifetime of the balloons; in other words, the “overseeding” factor.

The question arises as to whether the clustering is more pronounced on certain dates, i.e., for certain synoptic configurations, than on other dates. Because of the increase in clustering for the first 25–30 days after trajectory initiation, such a tendency could only be established through determination of the deviation from the mean clustering index 5, 10, 15 days, etc. after each trajectory initiation, and the averaging of these deviations by date. It turns out that the clustering index *does* tend to be above normal on certain dates, and figure 28 shows the autocorrelation coefficient derived from the variation of clustering with respect to date. The maximum in the autocorrelation coefficient suggests a clustering periodicity of about 45 days in winter and about 40 days in summer, though there is the confusing feature that the minimum in the coefficient occurs after a smaller time interval in the winter than in the summer. The difficulty is that we are trying to delineate a period not much shorter than the duration of the trajectories, and therefore, the periodicity can not be determined with accuracy. It must suffice to say that on the basis of these data there is a tendency for above-normal clustering to occur at intervals of slightly more than one month. The reason for such a periodicity remains obscure, since, as far as is known, there is no particular evidence for a monthly periodicity in other meteorological parameters (see, however, section 7 in this regard).

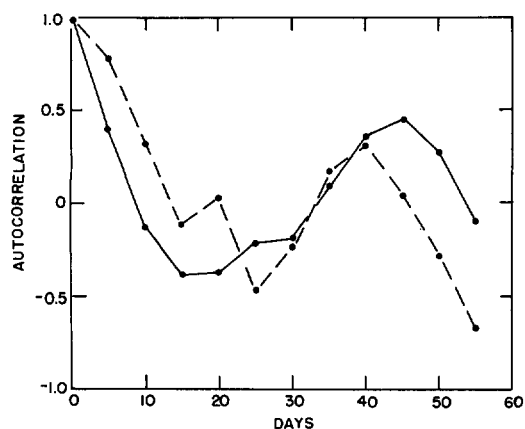


FIGURE 28.—Autocorrelation coefficient derived from the variation of the clustering index with respect to date, for winter (solid line) and summer (dashed line).

4. CLUSTERING AS A FUNCTION OF LATITUDE AND LONGITUDE

Also of importance from a practical point of view is the mean geographical location of regions of clustering and regions of particle sparsity, since the latter indicate where additional constant volume balloons might have to be released to maintain satisfactory data coverage. When dealing with the overall statistics it was possible, to some extent, to correct for the loss of particles to the Tropics, but of course it is impossible to estimate which particular grid squares the "lost" particles would be located within had they remained inside the NMC grid. Accordingly, this analysis concerning geographical coverage had to be carried out on the basis of the particles remaining within the grid. Figure 29 shows the mean particle density in winter and summer, 5–60 days after trajectory initiation, as well as the mean pressure-height patterns for these periods. Naturally, the loss of particles to the Tropics introduces a gradient in particle density directed toward the equator, and it is evident that any tendency toward clustering in latitude bands will be masked by this effect. Later on in this section we shall deal with this problem in more detail. For the moment let us consider the variation in particle density in the zonal direction. In winter, at any given latitude, the particle density is above average over western North America and, in particular, over Europe, with the maximum in particle density over Scandinavia. It is apparent that these maxima in particle density are associated with the mean ridges of pressure height, with some tendency for the particle density to reach a maximum just to the east thereof. The significance of this result is tempered by the fact that the particle density might be expected to be at a minimum to the east of the mean trough position, since the flow in that region is directed up the particle gradient. However, if this latter factor were the sole one acting there should be approximately a 90° phase lag between pressure-height

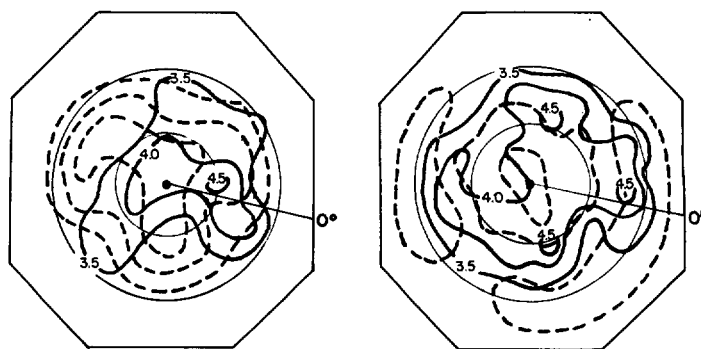


FIGURE 29.—Mean number of particles per 2,000-km. square, 5–60 days after trajectory initiation (solid lines), and the mean pressure-height field (dashed lines) for the corresponding period of winter (left) and summer (right). The circles represent latitudes 60° and 30° N.; the dot the North Pole.

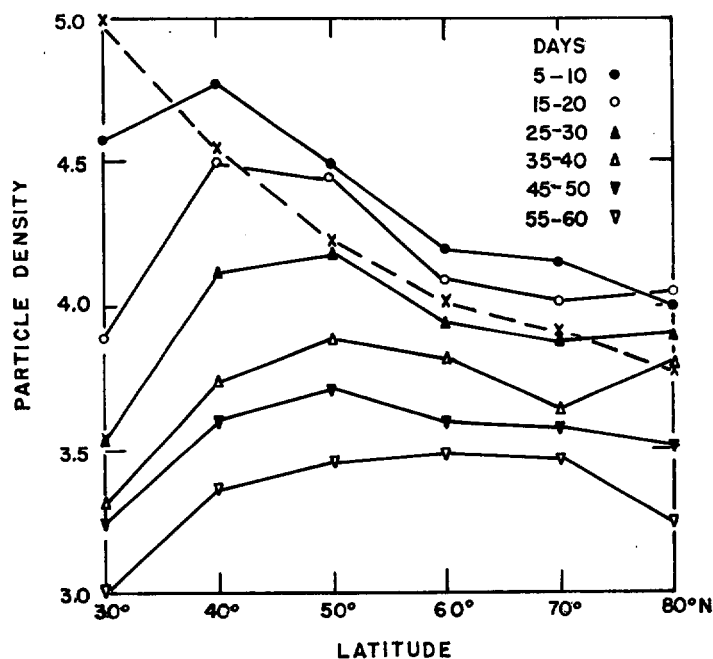


FIGURE 30.—Initial variation with latitude of the number of particles per 2,000-km. square (dashed line), and the mean particle density a given number of days after trajectory initiation (solid lines).

and particle density, and this is not observed. Consequently, there is probably some validity to the association of clustering with the ridges in pressure height and particle sparsity with the troughs in pressure height. Note that if this is true, on the average in winter the density of constant volume balloons would be relatively low just in the regions where they are most needed, namely, over the western Pacific and Atlantic Oceans.

In summer, there is little variation in particle density in the zonal direction, in agreement with the slight variation in pressure height. Contrary to the winter results, in summer the particle density is relatively high over the

North Atlantic and relatively low over Alaska. However, in both seasons it is obvious that the particle density is greater over Eurasia than over the remainder of the Hemisphere, and we shall have more to say about this in section 5.

With regard to the possibility of clustering in latitude bands, figure 30 presents a more detailed view of the variation of particle density with latitude. The dashed line represents the initial variation of particle density with latitude due to the overlaying of a square grid on a polar-stereographic map projection. When it is recalled that in addition, the particle density decreases to zero at 15° N., it is apparent why there is difficulty in determining whether or not a given density variation with latitude is due to a true clustering effect. Thus, the peaks at 40° and 50° N. in figure 30 have little significance since they would be bound to occur as a result of the loss of particles to the Tropics, coupled with the initial particle-density variation with latitude. However, on the basis of the slopes of the lines relative to the initial slopes, at least for the first 30 days, there is some evidence for clustering at 80° N. and, possibly, at 50° N., with a diminution in particle density at 60° – 70° N. Such a distribution is in general accord with the conventional 3-cell model in the meridional plane as long as 500 mb. is considered to be above the axes of the cells, as it generally is (see, for example, Mintz and Lang [4]).

In summary of this section, there is some evidence that, at 500 mb., the particle (constant volume balloon) density would be relatively low at the longitudes of the mean troughs (off the east coasts of the continents) and in the latitude band from 60° to 70° N. However, these results must be treated with caution because of the initial distribution of particle density with respect to latitude.

5. ZONAL VELOCITY OF AREAS OF CLUSTERING

Having discussed the mean variation of clustering with respect to geographical location, we now note how areas of clustering move with time. Visual inspection of figures 2–25 shows that the areas of clustering tend to move around the Northern Hemisphere in a counterclockwise sense. An attempt was made to place this movement on an objective basis through determination of the center of gravity, or the centroid, of the particle distribution. Figure 31 shows the successive positions of the centroid relative to the Pole for the winter and summer trajectories. In winter the centroid usually progresses in a counterclockwise sense, but frequently about a center displaced from the North Pole in the direction of the USSR. The displacement of the clustering centroid toward the USSR is in agreement with the previously noted correlation between clustering and pressure-height, and the tendency, emphasized by LaSeur [5], for the Northern Hemisphere vortex to be displaced toward Alaska. In the summer the situation is more chaotic and the counterclockwise circulation of the centroid sometimes gives way to a small-scale clockwise circulation. Note that the

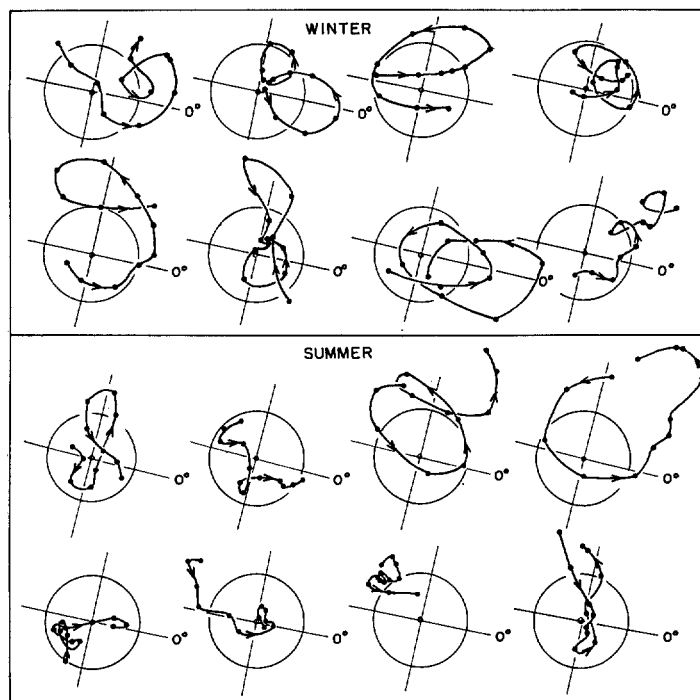


FIGURE 31.—Path of the clustering centroid relative to the North Pole based upon particle distributions at 5-day intervals for the eight trajectory initiations in winter (top) and summer (bottom). The circle represents latitude 88° N.

centroid is seldom displaced more than 5° latitude from the Pole in either season.

The displacement of the centroid circulation-center away from the Pole complicates the determination of the mean zonal speed of the clustering centroid. As a first approximation we have simply found the angular displacement of the centroid for each 5-day interval and averaged this (neglecting the direction of movement) for all trajectory starting times. Thereby, the average 5-day zonal displacement of the clustering centroid is found to be 38° longitude in winter and 32° longitude in summer, corresponding (at the representative latitude of 45° N.) to a mean zonal speed of 7 m. sec. $^{-1}$ in winter and 6 m. sec. $^{-1}$ in summer. The former value is close to the mean wave speed of 8 m. sec. $^{-1}$ determined by Johannessen and Cressman [6] from mainly wintertime maps. Thus, the clustering appears to be tied to the wave patterns, and to move with them on the average.

Through averaging of the centroid positions in figure 31 it is found that, 5 days after trajectory initiation, the clustering centroid is displaced toward the western North Pacific in winter and toward China in summer. The mean centroid position then moves eastward before stabilizing over the Russian Arctic. It is not completely clear why the clustering centroid initially is displaced in the general direction of Japan, although our best estimate is that this tendency reflects the strong divergent and convergent patterns associated with frequent cyclone development in this area.

6. CLUSTERING IN RELATION TO SYNOPTIC PRESSURE PATTERNS

It was shown in section 4 that in the mean there appeared to be a relation between particle density and pressure-height. However, there was some doubt concerning the validity of this result because of the initial gradient of particle density with respect to latitude. In order further to investigate this alleged relation, on individual dates the pressure-height field has been compared with the particle density. Figures 32 and 33 show such comparisons for the six middle dates (with respect to trajectory initiation and termination) in winter and summer. The particle density shown is an average one based on the particle density on the given date for each of the eight trajectory initiation times. In winter there is quite a strong tendency for clustering to occur on the ridges and for regions of low particle density to be located in troughs and low-pressure centers (Dec. 29 for example). On December 24, clustering is obviously associated with regions of weak pressure gradient. The extension upwind from the trough line of the region of particle deficiency on December 9 and December 14 suggests that meridional advection of the initial particle density is not the dominant criterion. In summer, on the other hand, no obvious relation between pressure pattern and particle density is evident from visual observation.

In order to place the above comparisons on an analytical basis, at every 10° of latitude a correlation was determined between pressure-height and particle density. In addition, at these same grid positions, the distance between contours was estimated and correlated with the particle density. Table 3 shows the correlations so obtained. Latitudes south of 40°N. were not utilized in the comparisons because of the probable effect of the loss of particles to the Tropics. During winter at latitudes 70° , 60° , and 50°N. there is a significant (at the 5 percent level, based on Fisher's Z test) correlation between pressure-height and particle density. In summer, however, the correlation is erratic. In winter at all latitudes there is a positive correlation between contour spacing and particle density. On the average this correlation is almost significant at the 5 percent level. In summer the latter correlation tends to be negative at the higher latitudes and positive at the lower latitudes, but none of the correlations is significant.

TABLE 3.—Correlation between pressure-height and particle density and, in parentheses, between contour spacing and particle density. The right hand column shows the correlation significant at the 5 percent level according to Fisher's Z test

Latitude	Winter	Summer	Significant Correlation
80°N.	0.08 (.05)	0.28 (−.14)	0.34
70°N.	.24 (.09)	.02 (−.10)	.24
60°N.	.35 (.06)	−.18 (−.10)	.20
50°N.	.28 (.15)	.08 (.12)	.19
40°N.	−.05 (.05)	−.14 (.04)	.18
Average	.18 (.08)	−.04 (−.02)	.10

The positive correlation between pressure-height and particle density in winter indicates that at 500 mb. there tends to be an ageostrophic inflow into ridges and high pressure centers and an ageostrophic outflow from troughs and low pressure centers. Insofar as pressure systems are vertical, this implies that 500 mb. is above the surface of non-divergence in the mean. The non-significant correlations in summer may indicate an upward movement of this surface of non-divergence. On the other hand, the positive correlation between contour spacing and particle density in winter tends to belie the concept of horizontal entrainment of particles into the jet stream, at least at the 500-mb. surface. Indeed, the jet stream may turn out to be a region where it is difficult to maintain a sufficient density of constant volume balloons.

7. DISPERSION STATISTICS

Certain dispersion statistics are readily obtainable from data of this type, and since the data are available for relatively long time periods and downwind distances, it is worthwhile to present some of these statistics. For political, as well as meteorological considerations, it is of interest to know the extent to which particle trajectories, initiated at a point, remain within a latitude band centered on that point, and the rapidity with which the particles extend to neighboring latitude bands. Inasmuch as we do not have enough separate trajectory initiations at a single point to yield good statistics, we have taken all the trajectories originating within a certain latitude band and have studied the latitudinal spread of these particles with time. Within the latitude band 55° – 65°N. there were 21 trajectory starting points, yielding for each season 168 separate trajectories. Figure 34 shows the percentage of particles remaining within the latitude band 50° – 70°N. a given number of days after trajectory initiation during winter and summer. After only five days, more than one-half of the particles have left this latitude band. In winter the proportion of particles remaining within the band after five days decreases nearly exponentially, but in summer there is a secondary maximum in the number of these particles 35–40 days after trajectory initiation. This suggests a large-scale meridional swaying of the atmosphere which may have some association with the periodicity in clustering noted earlier (fig. 28).

The top diagram of figure 35 shows the manner in which the particles initially in the latitude band 55° – 65°N. move equatorward. After 15 days the particle distribution is approximately Gaussian with respect to latitude, whereas after 60 days there are nearly equal numbers of particles in the 10° latitude bands between 50° and 20°N. Accordingly, after 15 days only 2 percent of the particles initially between 55° and 65°N. had passed equatorward of 20°N. whereas after 60 days 15 percent of the particles had passed south of that latitude. Such statistics may be of use in the estimation of the change in constant volume balloon height to be anticipated

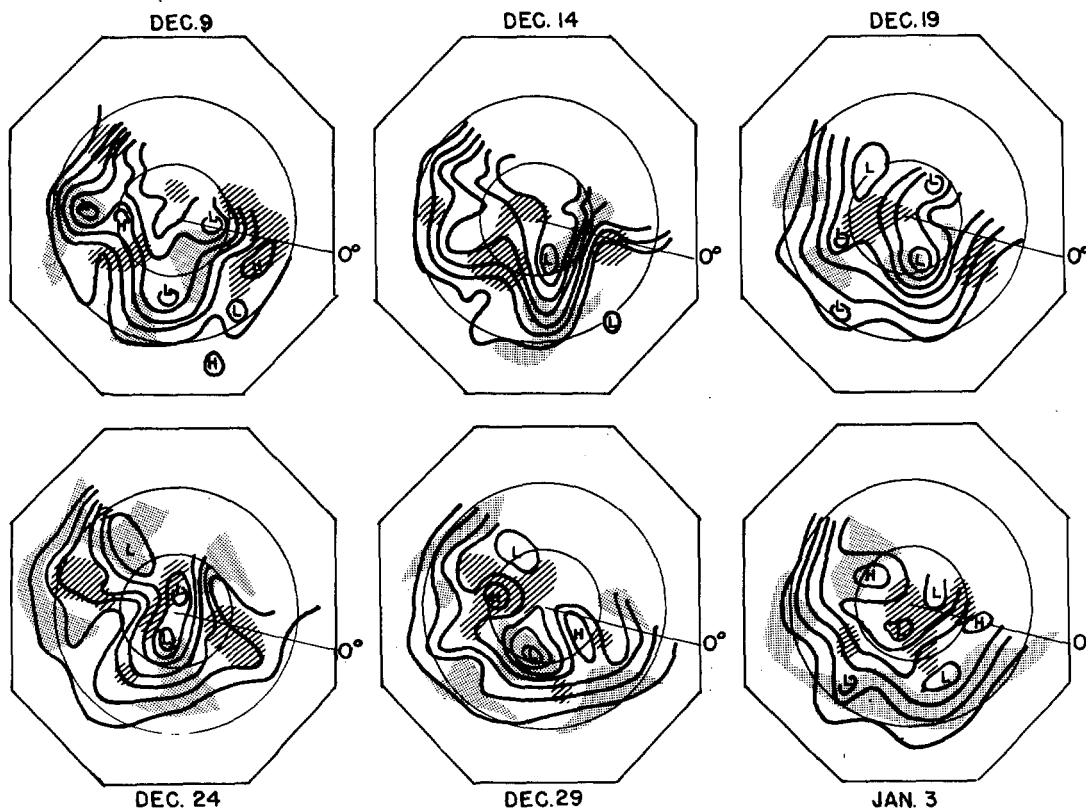


FIGURE 32.—Mean particle density (based on all eight trajectory initiations) superimposed upon 500-mb. pressure-height fields (solid lines) for the given dates in winter. Particle count exceeding 4.5 per 2,000-km. square delineated by hatching, less than 3.0 by stippling. The circles represent latitudes 60° and 30° N.

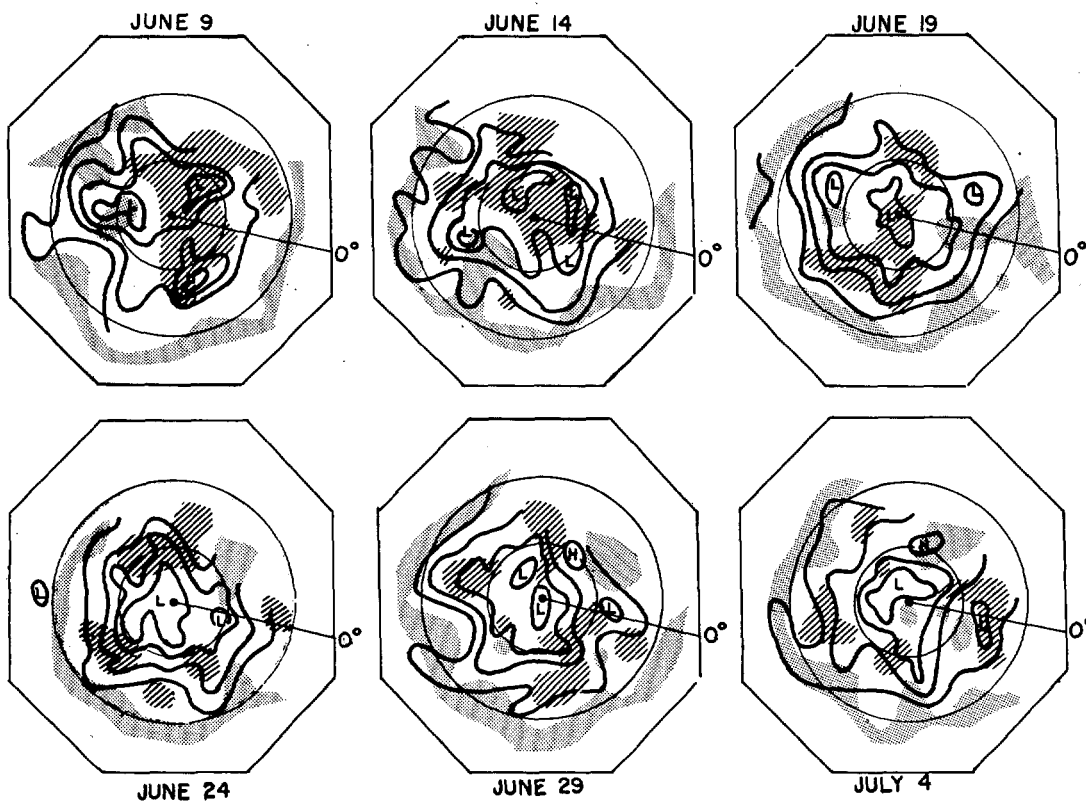


FIGURE 33.—Same as figure 32, but for trajectory initiations in summer.

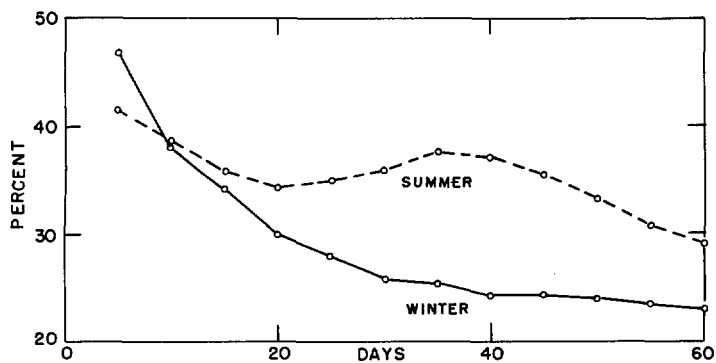


FIGURE 34.—Percentage of particles remaining within the 50–70° N. latitude band, a given number of days after trajectory initiation at grid points between 55° and 65° N.

because of latitudinal changes in the height of constant density surfaces.

The lower diagram of figure 35 shows the difference between winter and summer in this regard. As expected, there is generally a tendency for the particles to progress equatorward more quickly in winter than in summer with, for example, 10 percent more particles south of 40° N. in winter than in summer after 15 and 30 days. However, 60 days after initiation this tendency is reversed at all latitudes, implying that the meridional dispersion in summer, while slower, is more persistent.

Despite the fact that the number of particles does not have a truly Gaussian distribution with respect to latitude (particularly at the longer travel times), it is of interest to utilize these instantaneous “band source” data to estimate the magnitude of the lateral eddy diffusivity from the expression $K = \sigma_y^2 / 2t$, where σ_y is the latitudinal standard deviation and t is travel time. Substitution in the above equation for a travel time of 15 days (neglecting the fact that all trajectories do not originate at exactly the same latitude) gives values of 1.5 and 1.8×10^{10} cm.² sec.⁻¹ for the lateral eddy diffusivity in summer and winter, respectively. This is the same order of magnitude as derived by others from a variety of experiments. It should be noted, however, that the eddy diffusivity is only about half this value for a travel time of 60 days. Apparently, the latitudinal bounds on the data more than offset the usual tendency for the eddy diffusivity to increase with increase in travel time. This is not too surprising inasmuch as after 15 days of travel the particles should have sampled the largest scale of eddy existing in the atmosphere, and consequently, there would be little reason for K to continue to increase.

Durst and Davis [7] utilized geostrophic trajectories to study the variation with time of the separation distance between particles released simultaneously at different points. This was done for travel times as great as 36 hr. and for particles initially spaced from 80 to 560 km. apart. They found the separation distance to be proportional

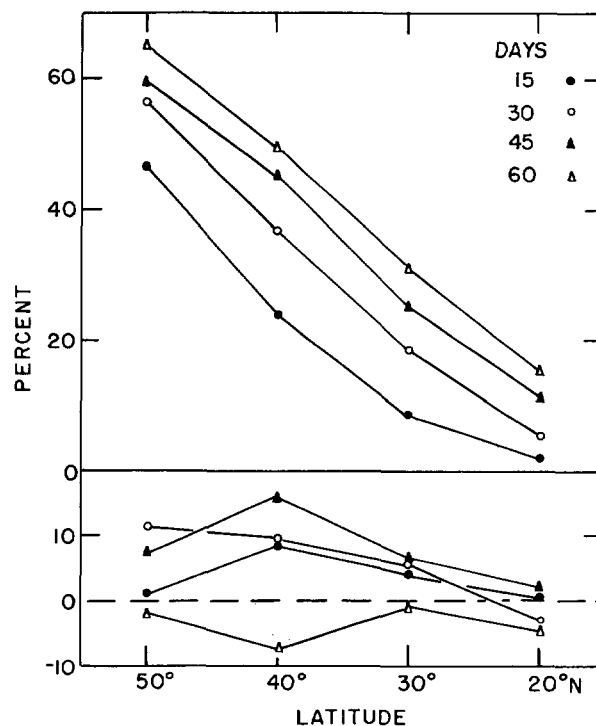


FIGURE 35.—Percentage of particles located south of the given latitude, a certain number of days after trajectory initiation at grid points between latitudes 55° and 65° N. (top), and the difference, winter minus summer (bottom).

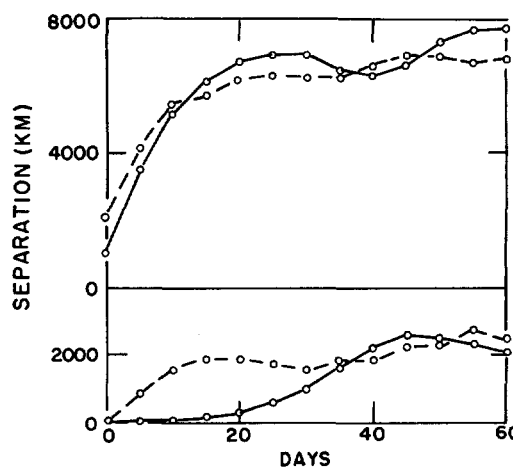


FIGURE 36.—Variation with time after trajectory initiation of the separation distance between particles initially 1,000 km. (solid lines) and 2,000 km. (dashed line) apart (top), and the difference, winter minus summer (bottom).

to the first power of the time and to the 0.86 power of the initial separation distance. Figure 36 shows the mean of our results for larger travel times, as based upon trajectories initiated from three points in the Japanese Islands, separated from each other by 1,000 km. For particles with an initial spacing of 1,000 and 2,000 km., the separation distance increases as about the 0.6 power of the time for the first 10 days, but thereafter the

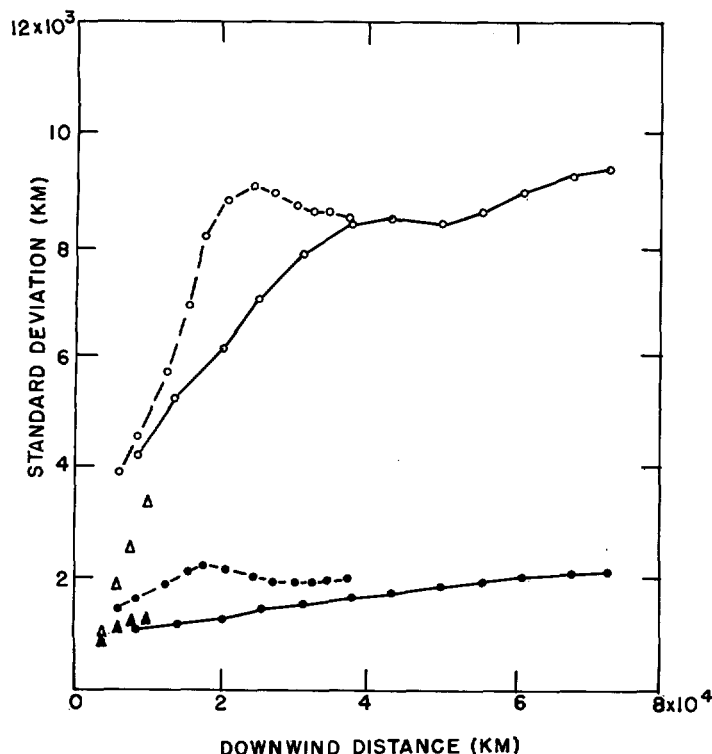


FIGURE 37.—Lateral (dots) and longitudinal (circles) standard deviation of particle positions (5, 10, 15, etc., days after trajectory initiation) as a function of downwind distance, based upon trajectories initiated at 5-day intervals from two sites in the Japanese Islands during winter (solid lines) and summer (dashed lines). Solid and open triangles show the results obtained by means of transosonde flights from Japan during fall, winter, and spring.

separation distance tends to stabilize at a value close to that of the earth's radius, or about 6,400 km. Furthermore, there is no evidence from our data that the subsequent separation distance is proportional to the initial separation distance, and thus it appears that the findings of Durst and Davis are not valid for periods as long as 5 days and/or separation distances as great as 1,000 km.

The lower diagram of figure 36 shows the difference in separation distance for winter and summer. As expected, the separation is always greater in winter than in summer, with the difference appearing to stabilize at a value of about one-third the average separation distance.

From the point of view of the diffusion to be expected from a "continuous" point source, it is worthwhile to study the variation with downwind distance of the lateral (and longitudinal) standard deviation of particles released from a given point at 5-day intervals. For this purpose, trajectories were initiated from Hokkaido and Okinawa in the Japanese Island chain and, as shown in figure 37, estimates of standard deviation were obtained for downwind distances as great as 70,000 km. in winter and 40,000 km. in summer, based upon the average zonal trajectory displacement for the 60 days. In winter the lateral standard deviation increases slowly but uniformly, with

the ratio of lateral standard deviation to downwind distance varying from 0.13, 5 days after trajectory initiation, to 0.03, 60 days after initiation. On the average in winter, then, the lateral standard deviation is proportional to about the 0.45 power of the downwind distance, not very different from the value of 0.5 expected in the limit for homogeneous turbulence. On the other hand, the longitudinal standard deviation increases much more abruptly, with the ratio of longitudinal standard deviation to downwind distance varying from 0.49, 5 days after initiation, to 0.13, 60 days after initiation. The longitudinal standard deviation is thus proportional to about the 0.65 power of the downwind distance in winter. Both standard deviations are larger in summer than in winter and, rather surprisingly, a maximum appears in both the summertime standard deviations at a downwind distance of about 20,000 km., or slightly less than the earth's circumference at middle latitudes.

For comparison with these results, in figure 37 are plotted the results obtained from constant level balloon (transosonde) flights from Japan during the fall, winter, and spring (Angell [3]). The lateral standard deviations obtained by the two methods collate quite nicely although, at a given downwind distance, the transosondes yielded a somewhat smaller longitudinal standard deviation than the hindcast NMC trajectories. Furthermore, even though the trajectories derived from the NMC historical tapes appear to furnish fairly representative dispersion statistics, presumably somewhat larger lateral standard deviations would have been obtained if the trajectory initiations had been at intervals of a few hours rather than a few days.

8. DATA COVERAGE FROM SPECIFIC LAUNCH SITES

One of the original purposes of this investigation was to estimate the data coverage to be expected from various constant volume balloon launch sites, and to determine the optimum configuration of launch sites. Unfortunately, it did not prove feasible to alter the computer program so as to obtain trajectories from only a single site, and consequently, because of the problem of computer time and cost, the statistics available consist solely of the eight trajectories initiated at 5-day intervals during a given season. Inasmuch as statistics obtained from such a small sample can hardly be considered representative, this problem is treated only briefly at this time.

It is logical that, during the initial stages of any such program, constant volume balloon launch sites in the Northern Hemisphere be located in or near Japan, since it is the North Pacific area that is most lacking in upper-air data. Consequently, in this study we chose as sites for trajectory initiation grid intersections located near the Islands of Hokkaido and Okinawa. Figure 38 shows the geographical distribution of grid squares, 2,000 km. on a side, which were traversed within the 60-day period by two-thirds (hatching) and one-third (stippling) of the

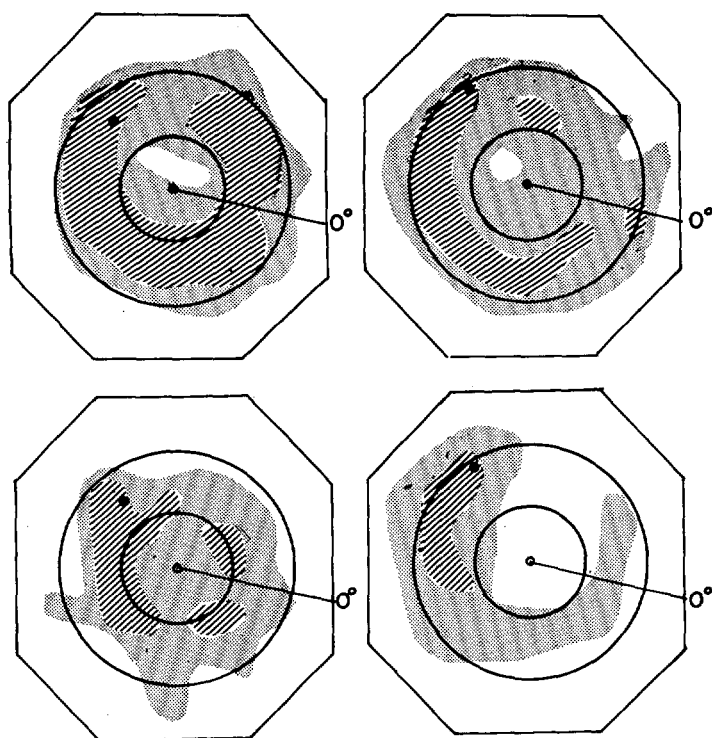


FIGURE 38.—Geographical distribution of 2,000-km. squares traversed by two-thirds (hatching) and one-third (stippling) of the trajectories initiated from Hokkaido (left hand diagrams) and Okinawa (right hand diagrams) during winter (top) and summer (bottom). The circles represent latitudes 60° and 30° N.

trajectories from each site during winter and summer. In general, as would be expected, data coverage tends to be good in the direction downwind from the launch site. However, note that while launches from Okinawa in summer would yield good data coverage over the southern North Pacific, they would not be at all effective in providing data over Eurasia. It is recognized that this type of information would be of considerably more use if our statistics were more numerous, and for this reason we will not deal further with this problem at this time. It should be mentioned that an alternative (Eulerian) method of providing statistics of this sort has been considered by Solot and Darling [8].

9. CONCLUSION

For at least two reasons, the statistics on clustering presented herein should be considered only as first approximations to the statistics which would actually be derived from a network of constant volume balloons. First, there is the question as to how well the velocity potential in the NMC model depicts the true ageostrophic flow in the atmosphere. Second, our results are almost certainly biased by the loss of particles to the Tropics. Only through actual experiments can the problem of clustering be solved with certainty, and for this reason it is hoped that the flying of constant volume balloons in the Southern Hemisphere (under the direction of Vincent Lally of the National Center for Atmospheric Research) can proceed as planned.

ACKNOWLEDGMENTS

The authors wish to thank Mr. George Dellert, now with Research Analysis Corporation, for the very great efforts he put forth in developing a suitable trajectory program. Most of the tedious hand work involved in this analysis, including the preparation of the particle-distribution diagrams, was performed by Mrs. Marguerite Hodges.

REFERENCES

1. V. E. Lally, "Satellite Satellites—A Conjecture on Future Atmospheric Sounding Systems," *Bulletin of the American Meteorological Society*, vol. 41, No. 8, Aug. 1960, pp. 429–432.
2. F. Mesinger, "Behavior of a Very Large Number of Constant-Volume Trajectories," *Journal of the Atmospheric Sciences*, vol. 22, No. 5, Sept. 1965, pp. 479–492.
3. J. K. Angell, "Use of Constant Level Balloons in Meteorology," *Advances in Geophysics*, vol. 8, Academic Press, New York, 1961, pp. 137–219.
4. Y. Mintz and J. Lang, "A Model of the Mean Meridional Circulation," *Investigations of the General Circulation of the Atmosphere*, Department of Meteorology, UCLA, March 1955.
5. N. E. LaSeur, "On the Asymmetry of the Middle-Latitude Circumpolar Current," *Journal of Meteorology*, vol. 11, No. 1, Feb. 1954, pp. 43–57.
6. K. R. Johannessen and G. P. Cressman, "Verification of an Equation for Trough and Ridge Motion," *Bulletin of the American Meteorological Society*, vol. 33, No. 7, Sept. 1952, pp. 267–273.
7. C. S. Durst and N. E. Davis, "Accuracy of Geostrophic Trajectories," *Meteorological Magazine*, vol. 86, No. 1019, May 1957, pp. 138–140.
8. S. B. Solot and E. M. Darling, "Theory of Large-Scale Atmospheric Diffusion and its Application to Air Trajectories," *Geophysical Research Papers*, No. 58, Air Force Cambridge Research Center, Bedford, Mass., June 1958 (3 volumes).

[Received November 3, 1965]